The inception and collapse of cloud cavitation in shock-structure interaction problems

Keita Ando[1]

[1]*Department of Mechanical Engineering, Keio University, Yokohama, Japan*

Keywords: Underwater explosion (UNDEX), fluid-structure interaction (FSI), cloud cavitation, heterogeneous cavitation inception, cavitation reloading

Abstract

In underwater explosions, the interaction of a shock wave with submarine structure often leads to strong tension in the liquid that can induce cloud cavitation. As a canonical example, we numerically study the dynamics of cloud cavitation that arises in one-dimensional, shock-structure interaction problems; an underwater shock is replicated using Cole's empirical formula and its interaction with a movable rigid plate (i.e., Taylor's free plate) is considered. The flow is modeled using homogeneous bubbly flow conservation equations in which interaction between bubbles and the averaged flow is incorporated through the mixture-averaged pressure field. To capture unsteadiness associated with bubble dynamics, the averaged equations are closed with a Rayleigh-Plesset-type equation. The resulting cloud cavitation is assumed to result from heterogeneous cavitation inception with single-sized, gas bubble nuclei. In solving the equations, a finite volume method with shock capturing is used and a time-step splitting technique is adopted to resolve stiffness owing to bubble-dynamic sources. One-dimensional cloud cavitation induced by the shock-structure interaction is simulated to clarify the fundamental mechanisms of the inception and the subsequent collapse of the cloud cavitation.

Introduction

Cavitation reloading on submerged structures is of great interest in underwater explosion (UNDEX) research (Rajendran, 2008). Fluid-structure interaction (FSI) often causes cloud cavitation near the target surface; the subsequent collapse of the cloud of cavitation bubbles can reload the target. In the pioneering study of Taylor (1941), the interaction of a plane shock with an infinite flat plate was considered and the linearized solutions that indicate the occurrence of negative pressure in (non-cavitating) liquids were obtained. Subsequently, the pressure cutoff model that assumes uniform pressure within cavitating regions was proposed to extend Taylor's classical theory (Kennard, 1950; Temperley, 1950). Bleich & Sandler (1970) assumed bilinear fluids and computed cavitation in Taylor's problem. More recently, Xie *et al.* (2007, 2009) employed a barotropic relation to describe the state of cavitation clouds, and simulated cavitation reloading on deformable structures. Although these cavitation models may replicate quasistatic trends in bubbly cavitating flows, it is not possible to properly capture unsteadiness and wave dispersion that arise from bubble dynamics (Brennen, 1995, 2005).

UNDEX/FSI experiments have been conducted by structural engineers (Nurick & Martin, 1989; Mair, 1999; Rajendran & Narasimhan, 2006*a*); one of the classical experimental configurations is a flat plate with shock loading due to detonation of high explosives. The photographs of Eldridge *et al.* (1950) illustrate a cloud of cavitation bubbles near a shock-loaded plate. Rajendran & Satyanarayana (1997) and Rajendran & Narasimhan (2006*b*) observed cavitation reloading from pressure and strain evolution on a deformed plate surface. Brett *et al.* (2000) and Brett & Yiannakopolous (2008) also confirmed the collapse of cavitation clouds adjacent to a submerged cylinder loaded from a nearby explosion.

Here, the dynamics of cloud cavitation that arises in one-dimensional UNDEX/FSI problems are numerically studied to clarify the fundamental physics of its inception and the subsequent collapse. In what follows, we review the classical UNDEX/FSI theories of Cole (1948) and Taylor (1941) and perform the modeling and simulation of a homogeneous bubbly flow in order to investigate averaged dynamics of bubbly cavitating mixtures.

Nomenclature

Roman letters

B	Tensile strength of a liquid (Pa)
C	Sonic speed of a liquid at a bubble wall (m s^{-1})
c	Sonic speed (m s^{-1})
H	Enthalpy of a liquid at a bubble wall (m^2 s^{-2})
m	Mass per unit area (kg m^{-2})
n	Bubble number density (m^{-3})
p	Pressure (Pa)
R	Bubble radius (m)
u	Velocity (m s^{-1})

Greek letters

α	Void fraction (−)
γ	Liquid stiffness (−)
ρ	Density (kg m^{-3})
τ	Time constant (s)
ψ	Taylor's FSI parameter (−)

Subscripts

0	Equilibrium values
b	Bubble quantities
l	Liquid quantities
p	Quantities of Taylor's plate
w	Quantities at bubble/plate walls

Problem Description

Consider the one-dimensional FSI problem of Taylor (1941) in which an UNDEX plane shock interacts with a movable rigid plate as depicted in Fig. 1. The shock pressure is assumed to show exponential decay with time constant τ (Cole, 1948). The plate is assumed to be "free" and "air-backed," meaning that the plate dynamics depend only on the pressure force from the water side.

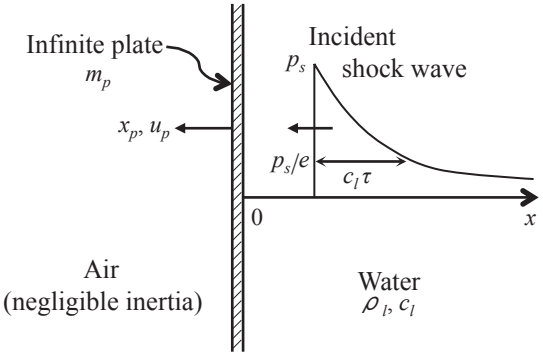

Figure 1: Schematic of the FSI model of Taylor (1941).

Let p_i and p_r be the pressures of the incident and reflected waves, respectively, at the plate wall (x = 0). Newton's second law requires

$$m_p \frac{du_p}{dt} = p_i + p_r , \tag{1}$$

where m_p is the mass of the plate per unit area and u_p is the plate velocity. Suppose that the acoustic relation holds (in case the water withstands tension without cavitation):

$$p_r = p_i - \rho_l c_l u_p , \tag{2}$$

where ρ_l is the water density and c_l is the speed of sound in the water. It follows from Eqs. (1) and (2) with $p_i = p_s \exp(-t/\tau)$, where p_s is the pressure at the shock front, that the evolution of the plate displacement is described by

$$x_p(t) = \frac{2p_s\tau^2}{m_p(1-\psi)}\left[\frac{1}{\psi}\left\{1-\exp\left(-\frac{\psi t}{\tau}\right)\right\}-\left\{1-\exp\left(-\frac{t}{\tau}\right)\right\}\right], \tag{3}$$

where the dimensionless FSI parameter, ψ, is defined as $\psi = \rho_l c_l \tau/m_p$. The final displacement is thus $x_p(\infty) = 2p_s\tau/(\rho_l c_l)$. The temporal evolution of the pressure on the plate wall is written as

$$p_{lw}(t) = p_{l0} + \frac{2p_s}{1-\psi}\left[\exp\left(-\frac{t}{\tau}\right)-\psi\exp\left(-\frac{\psi t}{\tau}\right)\right], \tag{4}$$

where p_{l0} denotes the ambient (equilibrium) pressure.

To interpret FSI effects on the pressure at the plate wall, its temporal evolution with varying the value of ψ in Eq. (4) is plotted in Fig. 2. It is confirmed that the wall pressure shows an instantaneous increase of the double incident shock strength at the collision time. Unlike the stationary wall case with its infinite inertia (ψ = 0), the plate motion yields tension (with negative pressures) in (non-cavitating) water; this tension has potential for inducing cavitation near the plate. Because the plate with smaller

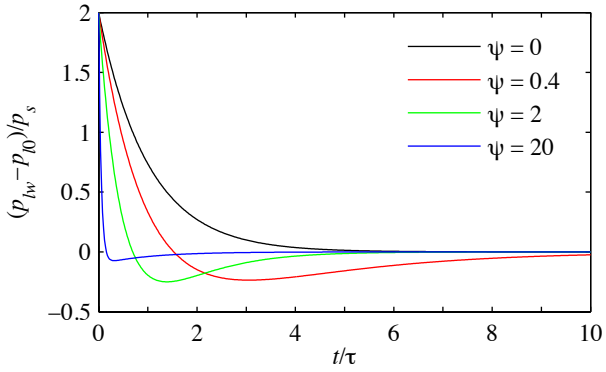

Figure 2: Evolution of the liquid pressure at Taylor's plate wall.

inertia more promptly responds to the shock loading, the time to achieve the minimum pressure decreases as the plate mass decreases. However, the duration of the tension part increases with increasing the plate mass. This suggests that the choice of Taylor's FSI parameter can control cavitation inception dynamics that depend strongly on the rate of change in liquid pressure to negative values.

What follows is to model mixture-averaged dynamics of bubbly cavitating flows in order to examine heterogeneous cavitation inception occurring in Taylor's FSI problem and the subsequent collapse of the cavitation cloud near the plate.

Physical Model

To study the averaged dynamics of cloud cavitation, we solve the ensemble-averaged conservation equations for homogeneous bubbly flows (for details of the model assumptions see Zhang & Prosperetti, 1994)

$$\frac{\partial\rho}{\partial t}+\frac{\partial(\rho u)}{\partial x}=0 , \tag{5}$$

$$\frac{\partial(\rho u)}{\partial t}+\frac{\partial}{\partial x}\left(\rho u^2+p_l-\tilde{p}\right)=0 , \tag{6}$$

$$\frac{\partial\alpha}{\partial t}+\frac{\partial(\alpha u)}{\partial x}=3\alpha\dot{R}^2 . \tag{7}$$

Here, ρ is the mixture density ($\approx (1-\alpha)\rho_l$), u is the mixture velocity, p_l is the averaged liquid pressure, $\tilde{p}$ represents pressure fluctuations due to the phase interaction (Ando *et al.*, 2011), α is the void fraction, and $\dot{R}$ is the bubble wall velocity (the dot denotes the substantial time derivative). The liquid pressure is described by the Tait equation of state (Thompson, 1972)

$$\frac{p_l+B}{p_{l0}+B}=\frac{1}{\rho_{l0}^{\gamma}}\left(\frac{\rho}{1-\alpha}\right)^{\gamma}, \tag{8}$$

where ρ_{l0} is the reference liquid density at p_{l0}, and γ and B denote stiffness and tensile strength of the liquid, respectively. The mixture is assumed monodisperse so that the void fraction is calculated as

$$\alpha=\frac{4\pi}{3}nR^3 , \tag{9}$$

where R is the bubble radius and n is the bubble number

density that is assumed spatially uniform at all times (i.e., no slip between bubbles and the host liquid). Note that for simulating cloud cavitation that originates from heterogeneous cavitation inception with air bubble nuclei, the initial void fraction of the cavitation nuclei is set to small values (say, $\alpha_0 = 10^{-5}$, representative value for tap water; Kedrinskii, 2005).

The homogeneous bubbly flow equations (5) to (7) are coupled to the equation of Gilmore (1952) that accounts for the effect of liquid compressibility on individual bubble dynamics:

$$R\ddot{R}\left(1-\frac{\dot{R}}{C}\right)+\frac{3}{2}\dot{R}^2\left(1-\frac{\dot{R}}{3C}\right)=H\left(1+\frac{\dot{R}}{C}\right)+\frac{R\dot{H}}{C}\left(1-\frac{\dot{R}}{C}\right), \quad (10)$$

where H and C are the enthalpy and the sonic speed of the liquid, respectively, at the bubble wall. The liquid pressure in Eq. (6) is now interpreted as the far-field pressure for the Gilmore equation (10); the flow is *two-way-coupled*. The two-way coupling assumption may be valid for dilute mixtures ($\alpha << 1$) in which direct interactions between the neighboring bubbles are negligible (van Wijngaarden, 1972). To efficiently evaluate effects of heat and mass transfer on bubble dynamics, the reduced-order model of Preston *et al.* (2007) is used to determine internal bubble pressure. Further details of the bubble-dynamic equations can be found in Ando *et al.* (2011).

For stable shock computations (LeVeque, 2002), the Gilmore equation (10) is put into conservation form:

$$\frac{\partial(nR)}{\partial t}+\frac{\partial(nRu)}{\partial x}=n\dot{R}\,. \quad (11)$$

In this form, the bubble radius is viewed as an Eulerian variable; the bubbles are considered to be distributed continuously in space.

Numerical Method

A finite-volume, fifth-order accurate, weighted essentially non-oscillatory (WENO) scheme (Liu *et al.*, 1994; Balsara & Shu, 2000), which has proven to work for accurate shock calculations in various examples (Shu, 1997), is used to reconstruct the conserved variables at cell edges from the cell-averaged quantities. The WENO reconstruction is performed in the characteristic space for shock calculations to be more robust (Qiu & Shu, 2002). The resulting local Riemann problem at each cell edge is solved using the HLLC Riemann solver (Toro *et al.*, 1994; Toro, 2009) so as to determine the numerical flux.

Since the system of the equations becomes very stiff in particular for the case of violently collapsing cavitation bubbles, a time-step splitting technique is adopted; the averaged fluid dynamics and the bubble dynamics are integrated separately in time in to tackle such stiffness. Here, the second-order accurate splitting scheme of Strang (1968) is used together with a third-order TVD Runge-Kutta (RK) scheme (Shu & Osher, 1988) and an adaptive RK scheme with time-step control (Press *et al.*, 1994), respectively, for the fluid-dynamic and bubble-dynamic parts.

FSI effects are incorporated into the model equations as reflecting boundary conditions. If the displacement of Taylor's plate is sufficiently small, the plate motion (Eq. (1)) can be incorporated at the fixed point ($x = 0$) in Eulerian

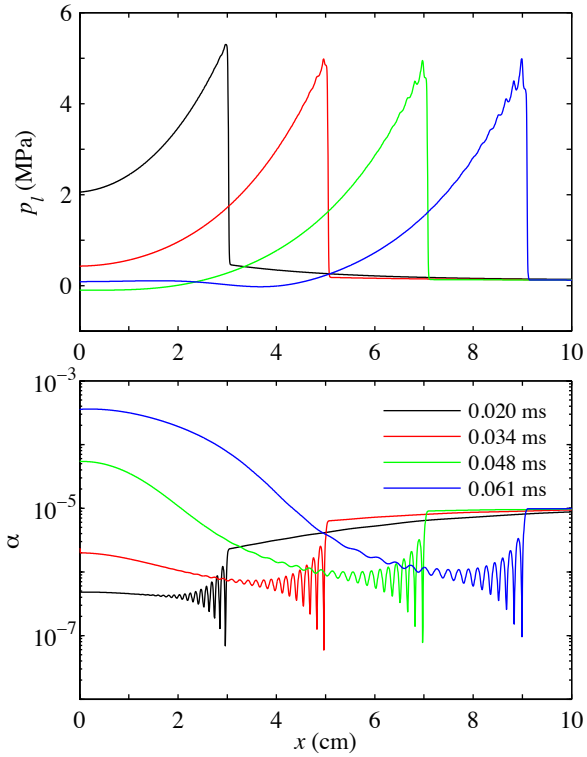

Figure 3: Spatial evolution of the averaged pressure (top) and the void fraction (bottom) for the UNDEX shock reflecting from Taylor's plate with $\psi = 0.1$. The time is measured from the shock collision with the plate at $x = 0$.

frame (LeVeque, 2002; Toro, 2009). Specifically, the small displacement condition is satisfied provided the final displacement $x_p(\infty)$ for non-cavitating liquids is far smaller than the relaxation length, $c_l\tau$, of Cole's UNDEX shock wave. To maintain the formal order of accuracy of the WENO reconstruction, we add extra fictitious cells away from the boundary (Dadone & Grossman, 1994).

The computational grid is uniform with cell width ($\Delta x = R_0$) and set to be large enough to prevent solutions of our concern near the plate wall from being contaminated with spurious waves reflected from the other boundary. The time step for the averaged fluid dynamics is set to be sufficiently small (CFL = 0.1) for splitting errors to be negligible.

Results and Discussion

As a model example, we simulate the experiment of Rajendran & Satyanarayana (1997) in which a steel plate ($m_p = 31.4$ kg m^{-2}) whose one side is covered with an air-filled tube was loaded by an underwater shock ($p_s = 4.98$ MPa, $\tau = 15.2$ μs) at the depth of 2 m from the free surface of water (20°C) with air bubble nuclei ($\alpha_0 = 10^{-5}$, $R_0 = 50$ μm); the induced fluid velocity corresponding to the shock pressure is according to the (linear) acoustic relation. Assuming that the tube attached to the plate is massless, the corresponding FSI parameter is computed as $\psi = 0.72$. For comparative purposes, the smaller value ($\psi = 0.1$), which may account for the effect of additional mass from the attached tube, is also considered. With these parameters, the small displacement condition is well satisfied so that the

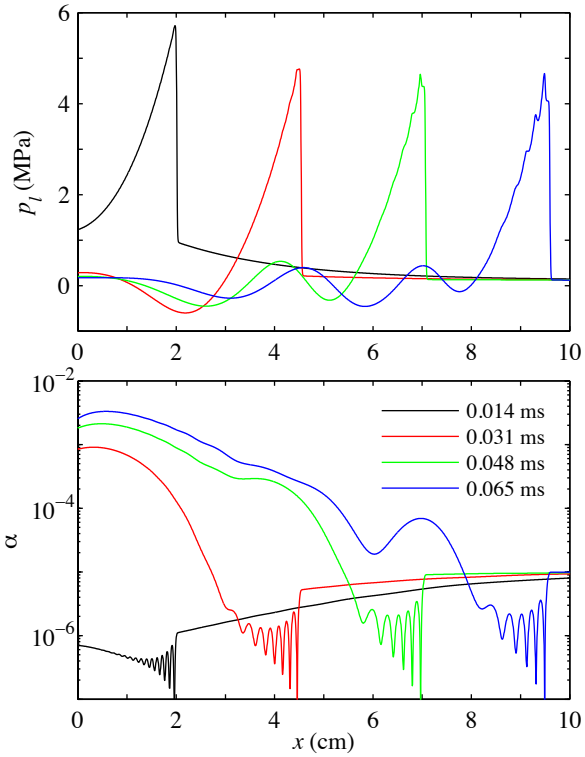

Figure 4: As Fig. 3, but with $\psi = 0.72$.

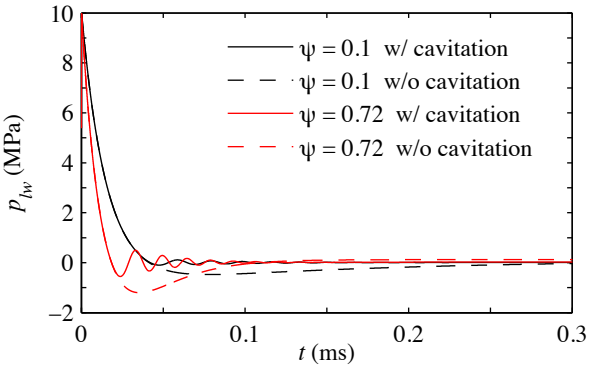

Figure 5: Temporal evolution of the averaged pressures at the plate wall in Figs. 3 and 4, together with the non-cavitating solutions (Eq. (4)) that exhibit minimum pressures at $t_{min} = 0.078$ ms and 0.036 ms for $\psi = 0.1$ and 0.72, respectively.

reflecting boundary conditions can be implemented in Eulerian frame.

In Fig. 3, we observe the evolution of the shock reflecting from the plate with $\psi = 0.1$ and the subsequent cloud cavitation. The air bubble nuclei are compressed by the reflected shock wave and show oscillations in volume behind the shock front. Despite the fact that the initial void fraction of the nuclei is as small as 10^{-5}, the sharp shock front exhibits decay and oscillations (in the averaged liquid pressure field) due to their bubble-dynamic effects as the shock evolves. The following tension wave leads to the growth of the cavitation nuclei neighboring the plate wall. The case with decreasing the plate inertia ($\psi = 0.72$) is presented in Fig. 4. Now that the plate responds to the loading more promptly, the relaxation tail of the shock shortens. As a result, the cloud expansion is more violent and the corresponding pressure rise is augmented.

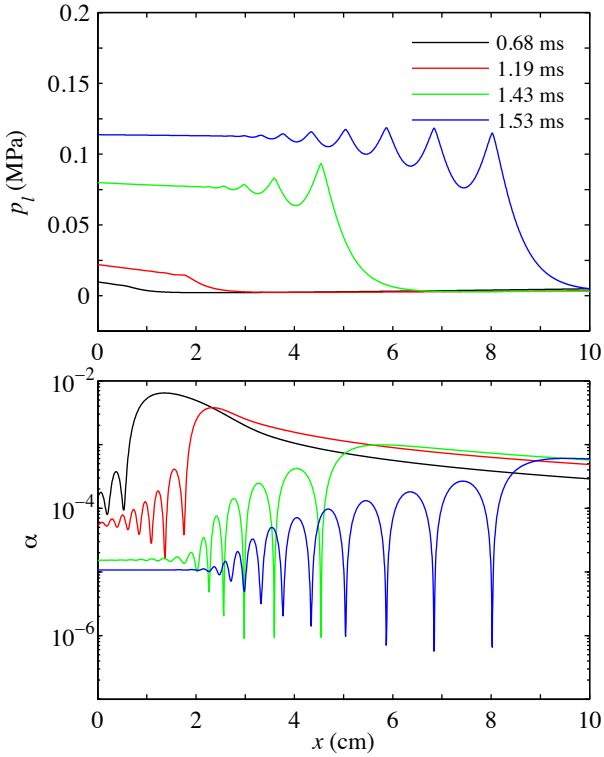

Figure 6: As Fig. 3 ($\psi = 0.1$), but for cloud collapse at later times.

The temporal evolution of the averaged pressure at the plate wall for the cases with $\psi = 0.1$ and 0.72 is presented in Fig. 5. For comparison, the non-cavitating solutions (Eq. (4)) are also plotted; the times at which the minimum pressures are encountered (denoted by t_{min}) are longer than the isothermal natural period of oscillations of the cavitation nuclei (0.017 ms). It is observed that the negative pressure (tension) duration substantially disappears due to cavitation caused by the structural interaction with $\psi = 0.1$. In this case, the decay time, t_{min}, is approximately five times as long as the period of bubble nuclei oscillations, so that the nuclei tend to respond to the ambient pressure variation in a quasi-static manner. In other words, the cavitation inception occurs immediately after the pressure falls below the vapor pressure. The tension wave with $\psi = 0.72$, on the contrary, leads to some negative pressure duration because of the inception delay. This example therefore suggests that in properly predicting heterogeneous cavitation inception with gas bubble nuclei (of representative sizes) in a liquid, there is a need to compare their oscillation periods with the duration of tension in the liquid.

The cavitation cloud in Figs. 3 and 4 begins to collapse and the shock forms and propagates from the plate as presented in Figs. 6 and 7, respectively. Note that the cloud collapse in the case of $\psi = 0.72$ starts earlier due to the observation that the pressure at the plate wall with increasing ψ returns to the ambient pressure p_{l0} more quickly in the non-cavitating case (see Fig. 2). The resulting shock pressure increases approximately to the ambient pressure as the shock evolves. Behind the shock front, the cloud exhibits oscillations in void fraction (or in volume). The cloud dynamics thus lead to oscillatory shock structure in the averaged pressure field; this is observed typically in shock propagation through monodisperse bubbly liquids

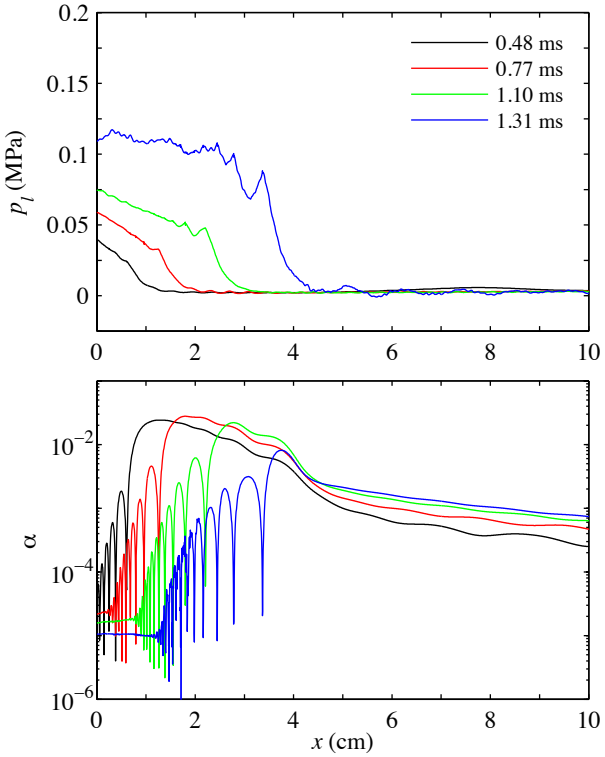

Figure 7: As Fig. 4 (ψ = 0.72), but for cloud collapse at later times.

(Ando *et al.*, 2013). It is more obvious in the case of ψ = 0.1 that the violent cloud collapse yields remarkable increase in the averaged pressure. However, the shock induced by the collapse is far weaker than the incident shock and cannot explain pronounced cavitation reloading as observed in Rajendran & Satyanarayana (1997). Hence, in this particular example, the one-dimensional cavitation cloud collapse is not violent enough to produce strong shocks that can account for the cavitation reloading. Furthermore, this indicates that geometric focusing effects in cavitation cloud collapse in two/three dimensions (Wang & Brennen, 1999; Wang, 1999) may be more important in the study of structural damage from cavitation reloading.

Concluding Remarks

The dynamics of one-dimensional cloud cavitation caused by structural interaction with an underwater shock were studied based on the homogeneous bubbly flow model with the classical theories of Cole (1948) and Taylor (1941). As a model problem, we simulated the experiment of Rajendran & Satyanarayana (1997). The heterogeneous cavitation inception is shown to be sensitive to the rate of change in liquid pressure to negative values (tension). If the duration of the tension state is sufficiently large compared with oscillation periods of gas bubble nuclei, the inception occurs immediately after the liquid pressure falls below the vapor pressure. It also transpires that the one-dimensional cloud collapse leads to oscillatory shock structure in the averaged pressure field but is not violent enough to produce strong shocks that can account for cavitation erosion.

In this paper the averaged cloud behavior in one dimension has been explored, while any scattering effects (such as fluctuations due to singe bubble collapse) in a specific realization of spherical bubbles. Quantification of the deviation from the averaged dynamics is of importance for cavitation erosion studies (Fuster & Colonius, 2012). Additional damping mechanisms associated with bubble fission (Brennen, 2002; Delale & Tunç, 2004) and bubble size distributions (Ando *et al.*, 2009, 2011, 2013; Colonius *et al.*, 2008) may play an important role for the averaged dynamics. These issues as well as the geometrical focusing effects need to be addressed in a future work.

Acknowledgements

The author would like to express his thanks to Professors Tim Colonius and Chris Brennen for their suggestions on this work, which was supported by ONR grant N00014-06-1-0730.

References

Ando, K. Colonius, T. & Brennen, C.E., Improvement of acoustic theory of ultrasonic waves in dilute bubbly liquids. Journal of the Acoustical Society of America, Vol. 126, EL69-EL74 (2009)

Ando, K., Colonius, T. & Brennen, C.E., Numerical simulation of shock propagation in a polydisperse bubbly liquid. International Journal of Multiphase Flow, Vol. 37, 596-608 (2011)

Ando, K., Colonius, T. & Brennen, C.E., *Shock Propagation in Polydisperse Bubbly Liquids*. In *Bubble Dynamics and Shock Waves, Shock Wave Science and Technology Reference Library (Vol. 8)*, 141-175, Springer (2013)

Balsara, D.S. & Shu, C.-W., Monotonicity preserving weighted essentially non-oscillatory schemes with increasingly high-order of accuracy. Journal of Compu- tational Physics, Vol. 160, 405-452 (2000)

Bleich, H.H. & Sandler, I.S., Interaction between structures and bilinear fluids. International Journal of Solids and Structures, Vol. 6, 617-639 (1970)

Brennen, C.E., *Cavitation and Bubble Dynamics*. Oxford University Press (1995)

Brennen, C.E., Fission of collapsing cavitation bubbles. Journal of Fluid Mechanics, Vol. 472, 153-166 (2002).

Brennen, C.E., *Fundamentals of Multiphase Flow*. Cambridge University Press (2005)

Brett, J.M., Yiannakopolous, G. & van der Schaaf, P.J., Time-resolved measurement of the deformation of submerged cylinders subjected to loading from a nearby explosion. International Journal of Impact Engineering, Vol. 24, 875-890 (2000)

Brett, J.M. & Yiannakopolous, G., A study of explosive effects in close proximity to a submerged cylinder. International Journal of Impact Engineering, Vol. 35, 206-225 (2008)

Cole, R.H., *Underwater Explosions*. Princeton University Press (1948)

Colonius, T., Hagmeijer, R., Ando, K. & Brennen, C.E., Statistical equilibrium of bubble oscillations in dilute

bubbly flows. Physics of Fluids, Vol. 20, 040902 (2008)

Dadone, A. & Grossman, B., Surface boundary conditions for the numerical solution of the Euler equations. AIAA Journal, Vol. 32, 285-293.

Delale, C.F. & Tunç, M., A bubble fission model for collapsing cavitation bubbles. Physics of Fluids, Vol. 16, 4200-4203 (2004)

Eldridge, J.E., Fye, P.M. & Spitzer, R.W., Photography of underwater explosions: I. In *Underwater Explosion Research (Vol. 1)*, 969-1052, Office of Naval Research (1950)

Fuster, D. & Colonius, T., Modelling bubble clusters in compressible liquids. Journal of Fluid Mechanics, Vol. 688, 352-389 (2011)

Gilmore, F.R., The collapse and growth of a spherical bubble in a viscous compressible liquid. Hydrodynamic Laboratory Report 26-4. California Institute of Technology (1952)

Kedrinskii, V.K., *Hydrodynamics of Explosions*. Springer (2005)

Kennard, E.H., Explosive load on underwater structures as modified by bulk cavitation. In *Underwater Explosion Research (Vol. 3)*, 227-253, Office of Naval Research (1950)

LeVeque, R.J., *Finite Volume Methods for Hyperbolic Problems*. Cambridge University Press (2002)

Liu, X.-D., Osher, S. & Chan, T., Weighted essentially non-oscillatory schemes. Journal of Computational Physics, Vol. 115, 200-212 (1994)

Mair, H.U., Benchmarks for submerged structure response to underwater explosions. Shock and Vibration, Vol. 6, 169-181 (1999)

Nurick, G.N. & Martin, J.B., Deformation of thin plates subjected to impulsive loading−a review (Part II: Experimental studies). International Journal of Impact Engineering, Vol. 8, 171-186 (1989)

Press, W.H., Teukolsky, S.A., Vetterling, W.T. & Flannary, B.P., *Numerical Recipes in FORTRAN: The Art of Scientific Computing*, Cambridge University Press (1994)

Preston, A.T., Colonius, T. & Brennen, C.E., A reduced-order model of diffusive effects on the dynamics of bubbles. Physics of Fluids, Vol. 19, 123302 (2007)

Qiu, J. & Shu, C.-W., On the construction, comparison, and local characteristic decomposition for high-order central WENO schemes. Journal of Computational Physics, Vol. 183, 187-209 (2002)

Rajendran, R. & Satyanarayana, K.H.B.S., Interaction of finite amplitude acoustic wave with a plane plate. Journal of the Acoustical Society of India, Vol. 25, V5.1-7 (1997)

Rajendran, R. & Narasimhan, K., Deformation and fracture behavior of plate specimens subjected to underwater explosions−a review. International Journal of Impact Engineering, Vol. 32, 1945-1963 (2006*a*)

Rajendran, R. & Narasimhan, K., A shock factor based approach for the damage assessment of plane plates subjected to underwater explosions. Journal of Strain Analysis for Engineering Design, Vol. 41, 417-425 (2006*b*)

Rajendran, R., Reloading effects on plane plates subjected to non-contact underwater explosion. Journal of Materials Processing Technology, Vol. 206, 275-281 (2008)

Shu, C.-W. & Osher, S., Efficient implementation of essentially non-oscillatory shock-capturing schemes. Journal of Computational Physics, Vol. 77, 439-471 (1988)

Shu, C.-W., Essentially non-oscillatory and weighted essentially non-oscillatory schemes for hyperbolic conservation laws. ICASE Report 97-65, NASA Langley Research Center (1997)

Strang, G., On the construction and comparison of difference schemes. SIAM Journal on Numerical Analysis, Vol. 5, 506-517 (1968)

Taylor, G.I., The pressure and impulse of submarine explosion waves on plates. In *The scientific papers of GI Taylor*, Vol. III, 287-303. Cambridge University Press (1941)

Temperley, H.N.V., Theoretical investigation of cavitation phenomena occurring when an underwater pressure pulse is incident on a yielding surface: I. In *Underwater Explosion Research (Vol. 3)*, 255-268, Office of Naval Research (1950)

Thompson, P.A., *Compressible-Fluid Dynamics*. McGraw-Hill (1972)

Toro, E.F., Spruce, M. & Speares, W., Restoration of the contact surface in the HLL-Riemann solver. Shock Waves, Vol. 4, 25-34 (1994)

Toro, E.F., *Riemann Solvers and Numerical Methods for Fluid Dynamics: A Practical Introduction*. Springer (2009)

van Wijngaarden, L., One-dimensional flow of liquids containing small gas bubbles. Annual Review of Fluid Mechanics, Vol. 4, 369-396 (1972)

Wang, Y.-C. & Brennen, C.E., Numerical computation of shock waves in a spherical cloud of cavitation bubbles. Journal of Fluids Engineering, Vol. 121, 872-880 (1999)

Wang, Y.-C., Effects of nuclei size distribution on the dynamics of a spherical cloud of cavitation bubbles. Journal of Fluids Engineering, Vol. 121, 881-886 (1999)

Xie, W.F., Young, Y.L., Liu, T.G. & Khoo, B.C., Dynamic response of deformable structures subjected to shock load and cavitation reload. Computational Mechanics, Vol. 40, 667-681 (2007)

Xie, W.F., Liu, Z.K. & Young, Y.L., Application of a coupled Eulerian-Lagrangian method to simulate interactions between deformable composite structures and compressible multiphase flow. International Journal for Numerical Methods in Engineering, Vol. 80, 1498-1519 (2009)

Zhang, Z.D. & Prosperetti, A., Ensemble-averaged equations for bubbly flows. Physics of Fluids, Vol. 6, 2956-2970 (1994)